Biogeochemistry **46:** 7–43, 1999.

Contemporary and pre-industrial global reactive nitrogen budgets

ELISABETH A. HOLLAND[1,2], FRANK J. DENTENER[3], BOBBY H. BRASWELL[4] & JAMES M. SULZMAN[1]

[1]*Atmospheric Chemistry Division, National Center for Atmospheric Research, Boulder, CO 80307 U.S.A.;* [2]*Max-Planck-Institut für Biogeochemie, D-00745 Jena, Federal Republic of Germany;* [3]*Utrecht University, Institute for Marine and Atmospheric Research (IMAU), Princetonplein 5, NL-3584 CC Utrecht, The Netherlands;* [4]*Institute for the Study of Earth, Oceans and Space, University of New Hampshire, Durham, NH 03824 U.S.A.*

Received 10 December 1998

Key words: ammonia emissions, global nitrogen cycle, nitric oxide, nitrogen deposition, nitrogen pollution

Abstract. Increases and expansion of anthropogenic emissions of both oxidized nitrogen compounds, NO_x, and a reduced nitrogen compound, NH_3, have driven an increase in nitrogen deposition. We estimate global NO_x and NH_3 emissions and use a model of the global troposphere, MOGUNTIA, to examine the pre-industrial and contemporary quantities and spatial patterns of wet and dry NO_y and NH_x deposition. Pre-industrial wet plus dry NO_x and NH_x deposition was greatest for tropical ecosystems, related to soil emissions, biomass burning and lightning emissions. Contemporary NO_y + NH_x wet and dry deposition onto Northern Hemisphere (NH) temperate ecosystems averages more than four times that of pre-industrial N deposition and far exceeds contemporary tropical N deposition. All temperate and tropical biomes receive more N via deposition today than pre-industrially. Comparison of contemporary wet deposition model estimates to measurements of wet deposition reveal that modeled and measured wet deposition for both NO_3^- and NH_4^+ were quite similar over the U.S. Over Western Europe, the model tended to underestimate wet deposition of NO_3^- and NH_4^+ but bulk deposition measurements were comparable to modeled total deposition. For the U.S. and Western Europe, we also estimated N emission and deposition budgets. In the U.S., estimated emissions exceed interpolated total deposition by 3–6 Tg N, suggesting that substantial N is transported offshore and/or the remote and rural location of the sites may fail to capture the deposition of urban emissions. In Europe, by contrast, interpolated total N deposition balances estimated emissions within the uncertainty of each.

Abbreviations: EMEP – European Monitoring and Evaluation Program; GEIA – Global Emissions Inventory Activity; NADP/NTN – National Atmospheric Deposition Program/National Trends Network in the U.S.; NH – Northern Hemisphere; $NH_x = NH_3 + NH_4^+$; $NO_x = NO + NO_2$; NO_y – total odd nitrogen = $NO_x + HNO_3 + HONO + HO_2NO_2 + NO_3$ + radical (NO_3^-)+; Peroxyacetyl nitrates + N_2O_5 + organic nitrates; SH – Southern Hemisphere; Gg – 10^9 g; Tg – 10^{12} g

Introduction

Inputs of nitrogen to terrestrial and aquatic ecosystems have increased several-fold over the last one hundred and fifty years, with the steepest increases during the last four decades. The expansion of fertilizer manufacture and use, the increase in fossil fuel combustion, the intensification of animal husbandry, and widespread cultivation of N_2 fixing crops have all contributed to the dramatic increase in N inputs. The increase has been most rapid in Northern Hemisphere (NH) temperate ecosystems, but presently subtropical and tropical regions of Asia are also experiencing an explosive increase in N inputs to terrestrial ecosystems (W. Chameides, pers. comm.; Galloway et al. 1996). Projected increases in N deposition for these tropical and subtropical regions, with a high natural background of N inputs, exceed increases projected for temperate and arctic regions (Cleveland et al. submitted; Galloway et al. 1994; Holland & Lamarque 1997a). Compared to biological N fixation, N deposition is becoming a proportionately greater source of N to terrestrial and aquatic ecosystems worldwide (Vitousek et al. 1997).

The nitrogen contained in the atmosphere as N_2, 3.9 * 10^6 Tg (Tg = 10^{12} g), is the largest reservoir of N in the Earth system (Warneck 1988). However, this paper focuses on the nitrogen emissions and deposition that have been transformed from N_2 into reactive forms that are biologically available (e.g. Vitousek et al. 1997). We consider the emissions of NO_x ($NO + NO_2$) and ammonia (NH_3) as well as their respective deposition products: NH_x ($NH_3 + NH_4^+$) and NO_y (total odd nitrogen, $NO_x + HNO_3 + HONO + HO_2NO_2 + RC(O)O_2NO_2 + NO_3^- + N_2O_5 + RONO_2$, where R is a higher alkyl group) (Ridley et al. 1996). Although deposition of all of these chemical species can be modeled, the deposition products most frequently measured are deposition of nitrate, NO_3^-, and ammonium, NH_4^+, in precipitation. Nitrate in rainwater is most commonly the dissolution product of nitric acid (HNO_3), but may also be the product of the dissolution of salts (e.g. $Ca(NO_3)_2$, $NaNO_3$, and NH_4NO_3), as well as organic nitrates. Ammonium is the dissolution product of compounds such as $(NH_4)_2SO_4$ and NH_4NO_3. There is increasing evidence that deposition of organic N may be important but there are few measurements (Cornell et al. 1995; Elkund et al. 1997; Rendell et al. 1993). Since there is little chemical interconversion between NO_x and NH_x in the atmosphere, on a global basis deposition of oxidized nitrogen (NO_y) and ammonia containing compounds (NH_x) will balance their respective emissions according to the law of mass conservation. The nitrogen-containing compound emitted (e.g. NO_x & NH_3) is not always the same as the compound deposited (e.g. HNO_3 and NH_x), but the nitrogen itself is conserved. The

aim of this paper is to examine the patterns, sources and magnitudes of pre-industrial and contemporary N deposition onto different ecosystem types.

Methods

To begin to understand how humans have changed N inputs to terrestrial ecosystems, we first used extant data to provide an up-to-date estimate of the global inventory of NO_x and NH_3 emissions. We then used a model of the troposphere, MOGUNTIA, to estimate N deposition inputs for both pre-industrial and modern scenarios (Dentener & Crutzen 1993; Dentener & Crutzen 1994). MOGUNTIA is currently the only global 3-D chemical transport model that simulates both NO_x emissions and its deposition (wet & dry) as NO_y, as well as NH_3 emissions and its deposition (wet & dry) as NH_x (Dentener & Crutzen 1994). In a previous study, MOGUNTIA-simulated NO_y deposition was similar to other models ranging in resolution from 2.4° by 2.4° up to the coarse resolution of 10° by 10° (Holland et al. 1997b). We then examined which vegetation types receive the wet and dry deposited N based on pre-industrial and contemporary vegetation distributions. Relatively clean Southern Hemisphere (SH) temperate ecosystems contrast strongly with NH temperate ecosystems, where human influence on N emissions and deposition is the greatest, and with tropical ecosystems where biological inputs and natural emissions of N containing trace gases are greatest.

Emission estimates

We reviewed the literature to construct global estimates of pre-industrial and modern emissions of the two most important classes of N emissions: NO_x and NH_3. The purpose of this exercise was: (1) provide a background against which to interpret the emissions used in the MOGUNTIA simulations, and (2) incorporate these newest estimates into the budget. A large number of global compilations of natural and anthropogenic NO_x-N emissions have been published recently (Benkovitz et al. 1996; Davidson & Kingerlee 1997; Delmas et al. 1997; Galloway et al. 1995; Holland et al. 1997b; Lee et al. 1997; Logan 1983; Prather et al. 1995; Price et al. 1997a; Price et al. 1997b; Sanhueza et al. 1995; Whelpdale et al. 1997). Two of the compilations, one of soil NO_x emissions and the other of global NO_x emissions, were the direct result of the SCOPE activity convened in Tsukuba, Japan in the spring of 1996 (Davidson & Kingerlee 1997; Delmas et al. 1997). A somewhat smaller number of contemporary global compilations of NH_3-N emissions have been published (Bottger et al. 1978; Bouwman et al. 1997; Dentener & Crutzen 1994; Galloway et al. 1995; Schlesinger & Hartley 1992; Soderlund

& Svensson 1976; Stedman & Shetter 1983; Warneck 1988). The most recent contemporary NH_3 emission inventory (Bouwman et al. 1997) is the most comprehensive.

Deposition estimates

Global estimates of total N deposition onto land were made using a model of the troposphere, MOGUNTIA, described by Zimmerman (1987) and modified by Dentener and Crutzen (1993, 1994). The modifications enable large scale modeling of atmospheric cycles of oxidized N: NO_x and NO_y, and reduced N: NH_3 and ammonium sulfate, $(NH_4)_2SO_4$. Like other 3-D chemical transport models, MOGUNTIA incorporates emissions of NO_x-N and NH_x-N (the latter is unique to MOGUNTIA) which are released on a latitude by longitude grid and transported. The sources of NH_3 and NO_x used in both the pre-industrial and contemporary runs are described in Tables 1 and 2. The emitted compounds undergo chemical transformation, and are then either deposited back to the surface as wet or dry deposition. We do not include surface emissions of nitrous oxide (N_2O), the largest source of surface-emitted N to the stratosphere, because it is unreactive in the troposphere. The primary mechanisms for NO_x-N, NO_y-N, and NH_x-N removal from the atmosphere are through wet deposition (via precipitation) and dry deposition of gases and particulates.

MOGUNTIA has a relatively coarse resolution of 10° by 10° grids; the modeled atmosphere extends from the surface to approximately 16 km and is divided into 10 layers of 100 hPa thickness (Zimmermann 1987). The model is driven using monthly average winds and temperatures from Oort (1983) and precipitation climatologies from Jaeger (1976). The time step of the photochemical portion of the model is two hours. Important features of the transport scheme include deep cumulus convection (Feichter & Crutzen 1990) and eddy diffusion based on the standard deviation of the monthly mean winds. The chemical species transported include NO_x, HNO_3, O_3, CO, CH_4, H_2O_2, H^+, SO_4^{2-}, NH_3, NH_4^+, CH_2O, DMS, SO_2, C_2-C_3^-, and peroxy-acetyl nitrate (PAN). The chemical scheme includes CH_4-CO-NO_x and HO_x with the associated photochemistry, heterogeneous destruction of N_2O_5, and the integration of sulfur and NH_x chemistry. Dry deposition is calculated according to

$$F = V_d n Y, \tag{1}$$

where V_d is the deposition velocity, n is molecules cm^{-3}, and Y is the mixing ratio of the gas. The deposition velocities are specific to the chemical species considered and vary depending on surface cover. The deposition velocities

Table 1. Global emissions of NO_x in Tg N y^{-1} to the troposphere for the mid 1800s and the 1980–90s compiled from a literature review (Benkovitz et al. 1996; Davidson & Kingerlee 1997; Delmas et al. 1997; Galloway et al. 1994; Holland et al. 1997b; Lee et al. 1997; Logan 1983; Prather et al. 1995; Price et al. 1997a; Sanhueza et al. 1995; Whelpdale et al. 1997). Values in parentheses are those used in the MOGUNTIA simulations described below (Dentener & Crutzen 1993; Dentener & Crutzen 1994).

Source	Pre-industrial	Contemporary
Fossil fuel combustion	0	20–24 (20)
Aircraft emissions	0	0.23–0.6 (0.6)
Biomass burning	0.25–7 (1.5)	3–13 (6.0)
Lightning	3–25 (5.06)	3–25 (5.06)
Soil NO_x emissions	3.59–18.2 (4.76)	4–21 (4.76)
Natural	4–15.5	4–15.5
Agricultural	?	1.8–5.4
NH_3 oxidation	0.2–0.6	0.5–3
Stratospheric injection	0.1–0.6 (0.5)	0.1–0.6 (0.5)
Total	7.8–41 (11.82)	23–81 (36.1)

Table 2. Global emissions of NH_x in Tg N y^{-1} to the troposphere for the mid 1800s and the 1980–90s (Bottger et al. 1978; Bouwman et al. 1997; Dentener & Crutzen 1994; Galloway et al. 1995; Schlesinger & Hartley 1992; Soderlund & Svensson 1976; Stedman & Shetter 1983; Warneck 1988). Values in parentheses are those used in the simulations described below (Dentener & Crutzen 1994).

Source	Pre-industrial	Industrial
Fossil fuel combustion	0	0.1–2.2 (–)
Industrial process	0	0.2 (–)
Domestic animal excreta		20–43 (22)
Biomass burning		2.0–8.0 (2.0)
Domestic animals + biomass burning	8.95 (8.95)	
Crops	(–)	3.6 (–)
Wild animal excreta	2.5 (2.5)	0.1–6 (2.5)
Synthetic fertilizer use	0	1.2–9.0 (6.4)
Oceans		8.2–13 (8.2)
Soils and natural vegetation	3.8 (3.8)	2.4–10 (5.1)
Humans and pets		2.6–4 (–)
Total	15–21 (15.2)	45–83 (46.2)

are: the NO_2 V_d over land is 0.25 cm s^{-1} and over the sea is 0.1 cm s^{-1}; the NO V_d over land is 0.04 cm s^{-1} and over the sea is 0.0 cm s^{-1}; the HNO_3 V_d over land is 2.0 cm s^{-1} and over the sea is 0.8 cm s^{-1}; the NO_3 V_d over land is 2.0 cm s^{-1} and over the sea is 0.8 cm s^{-1} (Dentener & Crutzen 1993); sulfate aerosols including $(NH_4^+)_2SO_4^{2-}$ have a deposition velocity of 0.1 cm s^{-1}, and dry deposition of NH_3 on land surfaces was calculated in the canopy using a temperature and biomass dependent canopy compensation point (Dentener & Crutzen 1994). Wet deposition is calculated according to

$$P = \frac{\epsilon R}{L}, \tag{2}$$

where P (s^{-1}) is the wet deposition rate constant, ϵ is dimensionless parameter correcting for less soluble species (for highly soluble species, $\epsilon = 1$); L (g m^{-3}) is the liquid water content of the rain cloud; R (g m^{-3} s^{-1}) is a function of R_0, the precipitation rate at the surface. R is calculated from R_0 using the function g (m^{-1}) describing the fraction of precipitation released at a given height interval calculated from the zonal mean data on the release of latent heat (Newell et al. 1974):

$$R(\phi, \lambda, Z, t) = R_0(\phi, \lambda, Z, t) \cdot g(\lambda, Z, t), \tag{3}$$

where ϕ is latitude, λ is longitude, Z is height and t is time. The following chemical species are subject to scavenging by precipitation: HNO_3, HNO_4, CH_2O, H_2O_2, CH_3O_2H, H_2SO_4, $(NH_4)_2SO_4$, SO_2, and NH_3. The gas phase species were corrected for their solubility using Henry's law coefficient.

This description of MOGUNTIA provides a basic overview of the model. More detail on how NO_x/NO_y and NH_x chemistry is implemented in the model is available in Dentener & Crutzen 1993 and 1994. The transport scheme and the photochemical schemes are described in Zimmerman 1987 and Crutzen & Zimmerman 1991. A comparison of the deposition scheme and simulated N deposition with the schemes and results of four other 3-D chemical transport models is available in Holland et al. 1997a.

Deposition measurements

We compared the wet deposition of NH_x and NO_y simulated by MOGUNTIA to wet deposition measurements from various sources. Although comparison with dry deposition data would have been valuable, dry deposition measurements are spatially and temporally sparse and most estimates of dry deposition rely on inferential models of dry deposition (Hicks 1989; Wesely 1989). By contrast, the network data used, NADP/NTN for the U.S. and EMEP for Europe, spanned 17 years of measurements at more than

350 sites and included measurement of precipitation necessary to calculate the wet deposition flux. We also compared the MOGUNTIA results to our recent compilation of NH_x and NO_3^- wet deposition measurements over the United States and Europe (Sulzman et al. 1997; Figure 1). We compared MOGUNTIA simulated deposition with the mean of all the sites which had measured the N deposition flux within a MOGUNTIA 10° by 10° grid cell. In addition, we compared the model to a global data set of wet deposition compiled by Dentener and Crutzen (1994).

In the United States, data on deposition inputs were provided by the National Atmospheric Deposition Program/National Trends Network (NADP/NTN, see *http://nadp.sws.uiuc.edu* for more information; Figure 1). Within the U.S., precipitation was collected in buckets which were triggered to open at the onset of rain, rather than using bulk precipitation collectors, which are subject to contamination and may sample significant amounts of dry deposition. Precipitation buckets were collected weekly at between 21–203 sites throughout the United States (average 156, although between 1985 and 1994, the number of sites was close to 200). All available measurements which met the criteria of: (1) more than 90% of the data had to have simultaneous measurement of both precipitation and chemistry and (2) more than 75% valid chemical measurements, were included in the spatial analyses. The precipitation was sent to a central laboratory for chemical analyses, including hydrogen ions (acidity as pH); associated anions: sulfate, nitrate and chloride; and base cations: ammonium, calcium, magnesium, potassium and sodium.

Wet deposition data for ammonium (NH_4^+) and nitrate (NO_3^-) for Europe were provided by the Cooperative Programme for Monitoring and Evaluation of the Long-Range Transmission of Air Pollutants in Europe (European Monitoring and Evaluation Programme, EMEP; Figure 1). In Europe, precipitation was collected daily using either the precipitation only samplers similar to those described above for the U.S. or bulk sampling devices which are continually open to the atmosphere. Forty three of the 108 sites used bulk precipitation collectors. Chemical analyses were done on a site by site or country by country basis rather than at a central laboratory. Across Europe, we used data from 108 out of the 188 sites which satisfied the same criteria for completeness described above. This filtering of EMEP data was done to enhance the comparability of the U.S. and European data sets. Some of the sites including Lazaropole, formerly Yugoslavia; Neuglobsow, Germany; Jarczew, Poland; Rarau, Seminic, Paring, Fundata, Turia, and Masun, Romania; and Ivan Sedlo, Bosnia-Herzegovina collected data monthly and the data should be viewed more critically. We used all available data reported for the time period 1978–1994. Data for 1994 are published as 'Data report 1994' by Anne Gunn-Hjellbrekke, Jan Schaug and

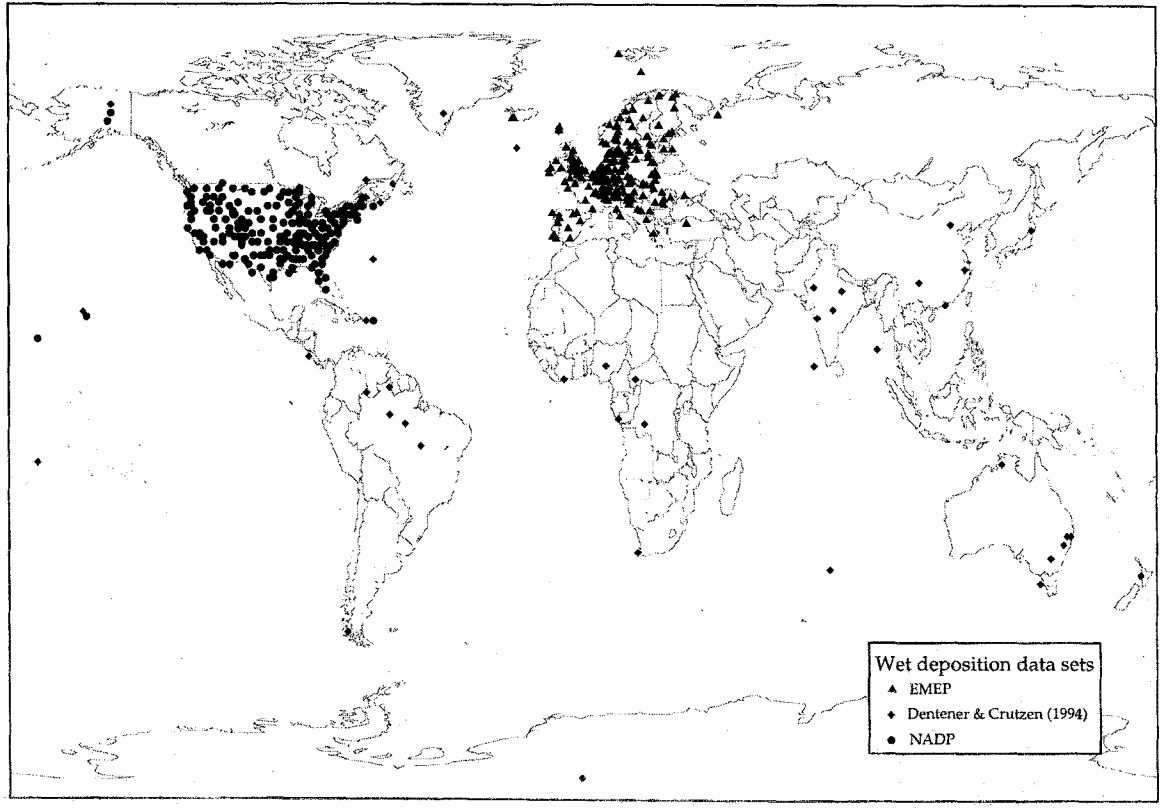

Figure 1. Map of wet deposition measurements sites used for comparison with the MOGUNTIA contemporary simulations. Three different networks were used: (1) the global network of data described in the Table 3 of Dentener and Crutzen, (2) NADP/NTN data for the U.S., and (3) EMEP network data for Europe. More details on the data and the networks is provided in the text.

Jan Erik Skjelmoen (EMEP/CCC 4/96), Kjeller, Norway 1996. Variations in collection procedures, analytical techniques, and the spatial coverage of the measurement sites as well as the representativeness of the site locations complicate the comparison across NADP and EMEP networks and amongst sites within the EMEP network. For both the European and U.S. data, we used data collected between 1978 and 1994.

To calculate the integrated deposition over the U.S. and Europe, we first mapped the wet deposition of NH_4^+ and NO_3^- by spatial interpolation of the annual mean site observations of wet deposition using moving window Kriging (Haas 1990) with precipitation and elevation covariates. The spatial interpolation (the Kriging analysis) was done using 237 sites for the wet deposition within the United States, and 108 sites for the wet deposition estimates within Europe. The spatial integration for Europe included both the bulk precipitation and wet-only deposition measurements. Some sites made measurements for only a few years, while others continued for the whole time period; thus, these numbers represent the total number of sites which made measurements in the 1978 and 1994 time period. For the U.S., we used gridded precipitation and elevation from the VEMAP Phase I data set (Kittel et al. 1995). This choice was made after evaluating the effects of using a wide range of covariates (including temperature, humidity, etc.) on Kriging model statistics. These statistics are based on a series of cross-validation studies in which each site in turn was withheld from the analysis, and the distribution of residuals (modeled minus predicted deposition) was examined. For Europe, we used precipitation and elevation from the Leemans and Cramer global data set (Leemans & Cramer 1991). All covariates and our desired output base map for both regions were defined on a 0.5° × 0.5° grid. To calculate the NH_x, NO_y and $NH_x + NO_y$ wet deposition over a region we summed the wet deposition in each of the grid cells. The same summation procedure was applied to the MOGUNTIA simulated deposition, after the output was regridded to the same 0.5° by 0.5° grid.

Vegetation maps

The type of vegetation receiving the N deposition is important to determining the ecological impact of the added N (Aber & Driscoll 1997; Aber et al. 1989). We used global maps of potential and present-day vegetation to examine the quantities of N being deposited on different biomes. For examination of pre-industrial N deposition onto terrestrial ecosystems, we use the potential natural vegetation map of Cramer et al. (1995), which is the same map used for global CENTURY simulations (Schimel et al. 1996; Schimel et al. 1997), and for estimation of global N_2 fixation (Cleveland et al. submitted). For examination of contemporary N deposition to terrestrial

ecosystems, we used the global map of vegetation distributions by DeFries and Townshend (1995). The vegetation classes used for the contemporary scenario included only 15 classes compared to 35 potential natural vegetation classes defined for the pre-industrial scenario.

The MOGUNTIA deposition fields and the DeFries and Townsend vegetation map were re-gridded to a 0.5° by 0.5° grid, without spatial interpolation or smoothing. For each half-degree cell a land cover type was assigned, and the deposition estimate was multiplied by the area of a vegetation type within each half-degree cell. We then calculated an areal-based summary deposition for each biome type on the common half-degree cells (Table 3).

Results and discussion

NO_x emissions

Emissions of oxidized N ($NO_x = NO + NO_2$) generate NO_3^- and NO_y deposition. The most common mechanism for NO_x removal from the troposphere is via the following reaction:

$$OH + NO_2 \longrightarrow HNO_3(g), \tag{4}$$

and via hydrolysis of N_2O_5:

$$N_2O_5 + H_2O \longrightarrow 2HNO_3, \tag{5}$$

Once formed, the HNO_3 is removed from the atmosphere via precipitation resulting in wet deposition. Gaseous HNO_3 may also be removed by dry deposition (Prather et al. 1995; Ridley & Atlas 1999).

Lightning, biomass burning and soil emissions of NO_x constitute the major sources of oxidized N in the pre-industrial atmosphere. Modeled NO_x fluxes from lightning and soil emissions are the same for the pre-industrial and contemporary time periods (Dentener & Crutzen 1994). Biomass burning NO_x fluxes are four-fold higher in contemporary simulations (Dentener & Crutzen 1994).

During the past decade, estimates of lightning production of NO_x have ranged from 2–100 Tg N y^{-1} (Table 1). Five 3-D chemical transport models that estimate deposition patterns based on emissions include global estimates of lightning production of NO_x ranges from a low of 3.0 Tg NO_x-N y^{-1} for GCTM (Levy et al. 1996a; Levy et al. 1996b) to a high of 10 Tg NO_x for GRANTOUR (Penner 1991; Penner 1994). The most recent estimates of

Table 3. Pre-industrial and contemporary N deposition onto biome types summarized from Tables 1 and 2 of the Appendix. The deposition is total deposition, $NO_y + NH_x$, and includes both wet and dry deposition simulated by MOGUNTIA (Dentener & Crutzen 1994). The land cover classification used for the pre-industrial scenario was the potential natural vegetation of Cramer et al. (1995). For the contemporary scenario, the land cover classification was the actual land cover described by Defries and Townshend (1994). The aggregation of vegetation types into biomes is indicated in the first column of Appendix 1, Tables 1 and 2. Ranges of deposition across vegetation types are provided in Appendix 1.

Biome	NH temperate latitudes			Tropical			SH temperate latitudes		
	N deposition $* 10^9$ g N	Area ha $* 10^9$	Average N deposition kg N ha^{-1}	N deposition $* 10^9$ g N	Area ha $* 10^9$	Average N deposition kg N ha^{-1}	N deposition $* 10^9$ g N	Area ha $* 10^9$	Average N deposition kg N ha^{-1}
				Pre-industrial					
Grasslands	**0.88**	*1.82*	0.50	**0.38**	*0.64*	1.42	**0.17**	*0.20*	0.63
Forests	**1.94**	*2.66*	1.02	**4.18**	*2.18*	1.85	**1.18**	*0.15*	0.76
Mixed	**0.82**	*1.70*	0.58	**2.77**	*2.09*	1.19	**0.51**	*0.80*	0.80
Life-forms wetlands & riparian zones	**0.37**	*0.66*	0.77	**0.31**	*1.48*	1.83	**0.01**	*0.02*	0.80
Ice	**0.02**	*0.05*	0.37				**0.00**	*0.00*	0.42
				Contemporary					
Grasslands	**6.39**	*2.42*	2.81	**2.87**	*1.99*	2.26	**0.32**	*0.62*	1.49
Forests	**9.47**	*2.58*	4.55	**4.94**	*1.49*	3.58	**0.19**	*0.10*	1.43
Mixed	**4.16**	*0.78*	6.20	**5.98**	*1.51*	3.94	**1.04**	*0.69*	1.85
Life-forms wetlands & riparian zones	**6.61**	*0.88*	7.42	**1.30**	*0.32*	4.15	**0.21**	*0.14*	1.54
Ice	**0.02**	*0.03*	0.55				**0.00**	*0.02*	0.05

lightning NO_x emissions of 12.2 and 13.2 Tg NO_x-N y^{-1} have been based on both lightning physics (Price et al. 1997a) and the global atmospheric electric circuit, respectively (Price et al. 1997b). Extrapolation of aircraft measurements made during thunderstorms in New Mexico, suggest global lightning emissions of 2.4–4.9 Tg NO_x-N y^{-1} between 8 and 12 km in altitude, but do not include the NO_x production rate below that altitude (Ridley et al. 1996). IPCC 1994 estimated lightning production of NO_x to be 8 Tg NO_x-N y^{-1} (Prather et al. 1995), while the 1994 Scientific Assessment of Ozone Depletion estimated lightning NO_x fluxes to be 7 Tg NO_x-N y^{-1} with a range of 3–20 Tg NO_x-N y^{-1} (Sanhueza et al. 1995), underscoring the uncertainty. There is substantial agreement that lightning emissions of NO_x lie somewhere between 3 and 25 Tg NO_x-N y^{-1}, with the most likely estimates falling between 10 and 15 Tg NO_x-N y^{-1}. This is considerable progress from a few years ago, when the estimates reached 100 Tg NO_x-N y^{-1} (Franzblau & Popp 1989).

Estimates of contemporary soil NO_x emissions range from 4–21 Tg NO_x-N y^{-1} (Table 1). Soil NO_x emission estimates used in five different global chemical transport models range from 4–10 Tg NO_x-N y^{-1} (Holland et al. 1997b), and some of the variability amongst the estimates can be explained by whether a soil NO_x-N emission estimate considers canopy uptake of NO_x. Both the ECHAM model estimate of 10 Tg NO_x-N y^{-1} and the MOGUNTIA estimate of 4.76 are based on the same studies (Galbally & Johansson 1989; Galbally & Roy 1978), but ECHAM neglects canopy scavenging of NO_x. Two models of soil NO_x-N emissions estimate the global soil NO_x flux to be 9.7 and 10.2 Tg NO_x-N y^{-1} (Potter et al. 1996; Yienger & Levy II 1995 respectively). The Yienger and Levy estimate was reduced to 5.45 Tg NO_x-N y^{-1} when parameterization of canopy scavenging was included in the simulation. However, a recent compilation of available measurements of soil NO_x-N emissions estimated below-canopy emissions of NO_x-N to be 21.2 Tg NO_x-N y^{-1} and above-canopy emissions of NO_x-N to be 13 Tg NO_x-N y^{-1} (Davidson & Kingerlee 1997). The likely error of the measurement compilation estimate is between 4 and 10 Tg NO_x-N y^{-1}. The error is attributable to uncertainties in estimated land areas, particularly for tropical woodlands and savannas, as well as a limited number of measurements in some biomes and vegetation types, particularly tropical agricultural ecosystems and deserts.

Production of NO_x-N related to biomass burning may be divided into two parts: that NO_x-N emitted during burning, and the NO_x-N emitted from the soil post-burning. Both fire-related sources of NO_x have increased with human activity. The emission of NO_x following biomass burning is neglected in most of the global compilations (both the soil and biomass burning portions of the budget), because clear documentation of the increase in flux and

its duration were measured only recently (Neff et al. 1995; Veldkamp & Keller 1997). The major sources of uncertainty associated with estimation of NO_x-N production during biomass burning are the quantification of the area burned, biomass burned, the timing and duration of the burn, and the amount of NO_x produced per unit of CO_2 released during the burn (Table 1). Crutzen and Andreae (1990) estimate 2.1 and 5.5 Tg NO_x-N y^{-1} emitted by biomass burning globally, with the greatest contribution by tropical fires. In 1987, burning in the Amazon alone contributed 1 Tg NO_x N y^{-1} (Setzer & Pereira 1991). A current inventory of biomass burning fluxes of both NO_x and NH_3 is underway as part of the Global Emissions Inventory Activity (GEIA, *http://blueskies.sprl.umich.edu/geia/*). Estimates of modern day contributions of biomass burning to the global NO_x-N budget differ by 4-fold (Table 1) and the pre-industrial estimates of biomass burning contributions range from 0.25 to 7 Tg NO_x-N y^{-1}, an even greater range. The difficulty of quantifying the area and biomass burned is a problem for both the pre-industrial and contemporary estimates of NO_x and NH_3 emissions.

Combustion of fossil fuel and aircraft NO_x emissions are by-products of industrialization, and have increased from almost 0 in the last century to between 20 and 25 Tg N for the last two decades. Ninety percent of industrial NO_x emissions originate from countries located at northern temperate latitudes (the U.S., Canada, Western and Eastern Europe, the Former USSR, China, Japan, and the Middle East) (Olivier et al. 1995). The energy statistics and emission factors (NO_x per unit CO_2 emitted) used to quantify fossil fuel combustion for both NO_x and CO_2 are known, but the emission factors vary by an order of magnitude from fuel type to fuel type. Uncertainty arises from limitations of reporting fossil fuel consumption statistics on a country by country basis, and the re-gridding necessary for use in 3-D global models. The differing years for which statistics are reported also contribute to the uncertainty. There have been a number of global compilations of fossil fuel NO_x emissions (Benkovitz et al. 1996; Dignon & Hameed 1989; Logan 1983; Muller 1992). The Benkovitz et al. (1996) compilation is available through GEIA (*http://blueskies.sprl.umich.edu/geia/*). Uncertainties for fossil fuel NO_x emissions remain $\pm 30\%$, and may be as high as 50% for some regions of the world (Lee et al. 1997). Uncertainties for the potentially large natural sources (e.g. biomass burning, lightning and soil emissions), remain at $\pm 100\%$ and greater as shown here (Table 1).

NH_3 emissions

NH_x exchanges are important because of their magnitude (Table 2). NH_3 is involved in aerosol formation, plays a central role in the global nitrogen cycle, and is the most abundant atmospheric base with the ability to neutralize

harmful acids. In addition, when NH_3 or NH_4^+ is oxidized in soils, through nitrification, acidifying hydrogen ions are liberated (van Breemen et al. 1982). Estimates of global NH_3 emissions exceed those for NO_x (Bottger et al. 1978; Bouwman et al. 1997; Dentener & Crutzen 1994; Galloway et al. 1995; Schlesinger & Hartley 1992; Soderlund & Svensson 1976; Stedman & Shetter 1983; Warneck 1988). Fossil fuel contributions to global NH_3 emissions are small, but domestic animal excreta dominates both the pre-industrial and contemporary NH_3 budgets (Table 2). Present day domestic animal populations are quantified to within 10%, but pre-industrial estimates rely on extrapolations through time based on a much sparser data set or by analogy to the better quantified human population (Bouwman et al. 1997; Olivier et al. 1995). The total estimate of uncertainty for NH_3 emissions from domestic animal excrement is $\pm 50\%$, which is reflected in the range of the estimates in Table 2. Emission of NH_3 from well fertilized crops and from soils following the application of animal waste and synthetic fertilizer is substantial. The percentage of fertilizer returned to the atmosphere as NH_3 varies between 2 and 30% depending on the type of fertilizer, soil characteristics, and fertilizer management, particularly the timing method of application. Although, fertilizer use is well quantified (FAO 1985; Matthews 1994), estimates of NH_3 emissions following fertilization vary (Bouwman et al. 1997; Warneck 1988). Furthermore, the most recent estimates of 5–9 Tg N y^{-1} are much greater than the previous estimates of 1.2–3.5 Tg N y^{-1} (Bottger et al. 1978; Crutzen & Gidel 1983; Stedman & Shetter 1983; Warneck 1988), and the differences cannot be explained by the rise in fertilizer use between the two sets of estimates. Crop emissions are estimated to be 2.5 kg N ha^{-1} for all arable land. The extensive data available for NH_3 emissions from a wide array of industrial processes including fertilizer and chemical manufacture allow for the robust determination of a rather small number (Bouwman et al. 1997). Estimation of NH_3 emission by fossil fuel combustion is limited by the availability of algorithms for different fuel types, but the most recent estimate of Bouwman et al. (1997) is quite low at 0.1 Tg N y^{-1} with an uncertainty of 0.0–0.3 Tg N y^{-1}. All animals, including humans and their pets, emit NH_3 in their breath and sweat. The latest global estimate of 2.6 Tg N y^{-1} (Bouwman et al. 1997) assumed an emission of 0.5 kg N $person^{-1}$ (or animal) y^{-1}. Agriculture contributes more than 50% of the NH_3 emissions globally. Emissions of NH_3-N from sub-tropical and tropical latitudes are much more important than they are for global NO_x-N, which are dominated by Northern Hemisphere fossil fuel emissions.

As with the NO_x emissions budgets, quantification of the natural sources of NH_3, including emissions of NH_3 from the excreta of wild animals, soils and natural vegetation, and the ocean, are uncertain, and estimates vary

by two to four-fold. These natural sources comprise the pre-industrial NH_3 budget and so their uncertainty dominates estimation of pre-industrial NH_3 emissions. Many factors contribute to the uncertainty. Wild animal population censuses are rare and global censuses even rarer (Bouwman et al. 1997). Soil and vegetation NH_3 emission estimates are complicated by plant scavenging of atmospheric NH_3. Over the course of a few days, plant uptake can completely counterbalance emissions (Langford et al. 1992). Global soils emissions have been estimated as high as 38 Tg N y^{-1} (Dawson 1977) but it is unlikely that all of the NH_3 emitted escapes to the atmosphere (Warneck 1988). Oceanic emissions estimates suffer the same problem as plant and soils emission because NH_3 may be either consumed or emitted (Bouwman et al. 1997). Thus, the sole estimate of pre-industrial NH_3 emissions made by Dentener and Crutzen (1994) is highly uncertain. A complication is the extent to which natural emissions and associated deposition of NO_x and NH_3 from soils/vegetation and biomass burning represent a net input into an ecosystem.

Modeled nitrogen deposition

Simulated pre-industrial N deposition was greatest over tropical ecosystems according to the MOGUNTIA simulations (Figure 2; Dentener & Crutzen 1994). Rates of total N (NH_x + NO_y) deposition ranged from 0–3.1 kg N ha^{-1} y^{-1} before industrialization with the highest rates of deposition in northwestern South America, Central Africa, and Southern Asia including the Indonesian Islands. Total NH_x deposition was highest over northeastern South America, and greater than 0.5 kg ha^{-1} over large areas of tropical Africa, South America, and Asia, and less than 1 kg N ha^{-1} for both northern and southern temperate ecosystems. Total NO_y deposition was greatest in Central Africa, greater than 0.75 kg N ha^{-1} over most of the tropical land mass, and less than 1 kg N ha^{-1} for both northern and southern temperate ecosystems. These high rates of pre-industrial N deposition onto tropical latitudes are driven by biomass burning and soil emissions of NO_x and NH_3 as well as lightning production of NO_x, all of which are greatest in the tropics (Holland 1997a). Thus, the pre-industrial pattern of high emissions and deposition at tropical latitudes causes a continental scale recycling of N in ecosystems where the only other source of N is via biological N_2 fixation. However, the rates of N fixation for tropical ecosystems are estimated to be between 10 and 20 kg N ha^{-1} y^{-1} (Cleveland et al. submitted), 10 times the average pre-industrial N deposition.

Pre-industrial and contemporary total N deposition had strikingly different magnitudes and spatial patterns (Figures 2 and 3). In contrast with the tropical distribution of the greatest pre-industrial total N deposition, contemporary total N deposition is greatest at northern temperate latitudes (Figures 2 and

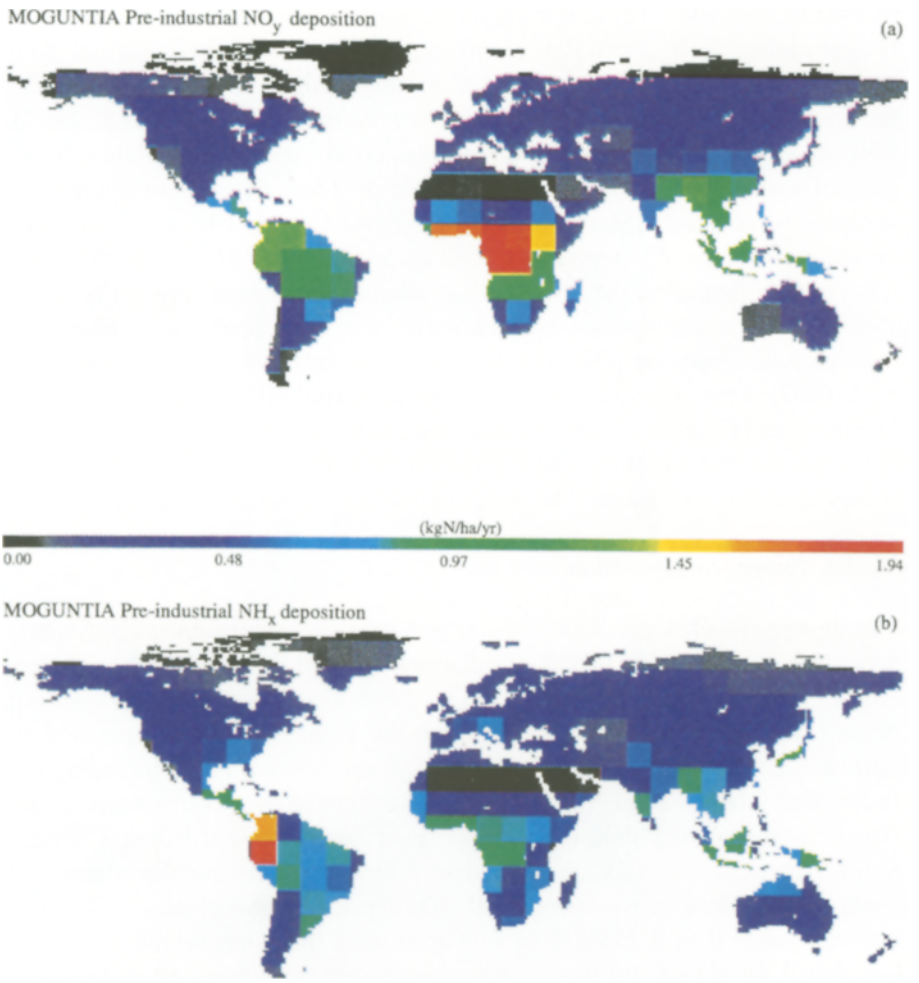

Figure 2. Modeled pre-industrial wet and dry NO_y-N deposition (a) and NH_x-N deposition (b) deposition onto terrestrial ecosystems. The results were generated using a model of the troposphere, MOGUNTIA (Dentener & Crutzen 1994).

3; Table 3; Appendix 1; Dentener & Crutzen 1994). Across all of the biomes at tropical and temperate latitudes, contemporary total N deposition exceeds pre-industrial total N deposition (Table 3). The northern temperate biomes most affected by total N deposition, cultivated lands and mixed forests, receive >16 times more N today than they did a century ago according to the MOGUNTIA simulations. On average, there was more than a four-fold increase in the rates of N deposition onto NH temperate ecosystems for the contemporary compared to the pre-industrial scenario. The increase in nitrate concentration in NH ice cores shows a similar increase over the last century

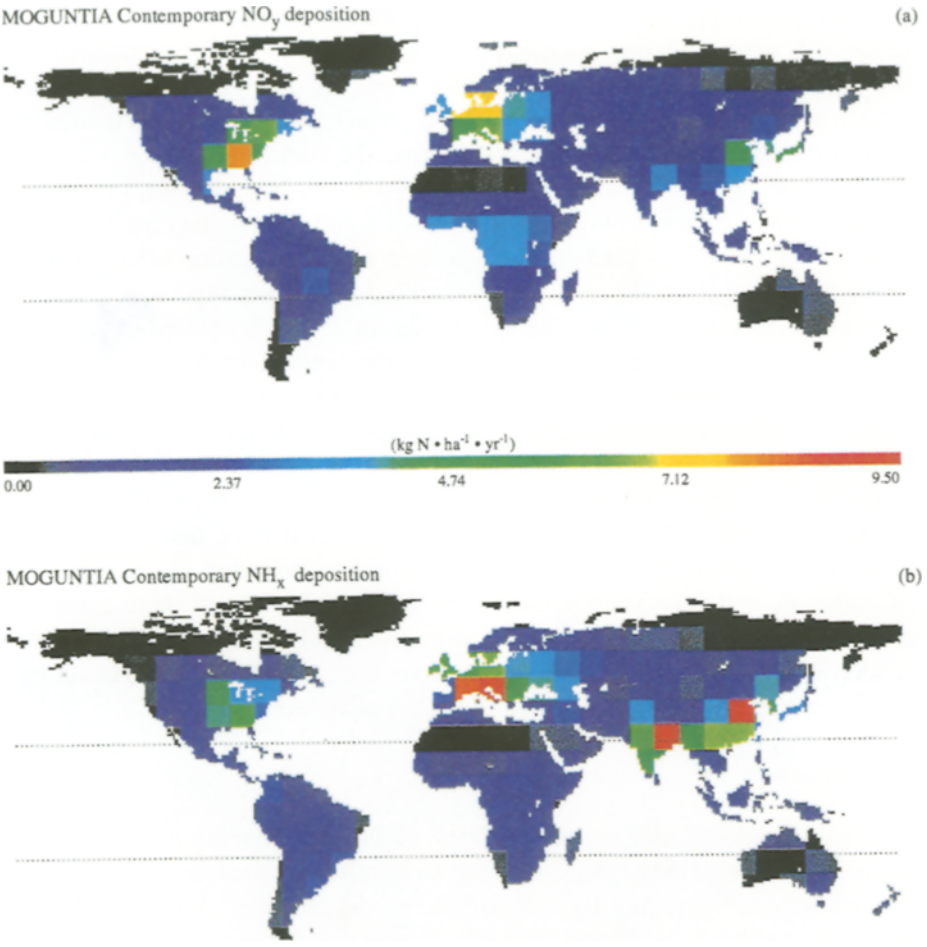

Figure 3. Modeled contemporary wet and dry NO_y-N deposition (a) and NH_x-N deposition (b) deposition onto terrestrial ecosystems. The results were generated using a model of the troposphere, MOGUNTIA (Dentener & Crutzen 1994).

(Mayewski et al. 1990; Wagenbach et al. 1988). Total NO_y deposition exceeds 10 kg N ha^{-1} y^{-1} over the Eastern U.S. and Western Europe, which are among the most industrialized regions of the modern world. Southern Asia, one of the fastest developing regions of the world, is receiving more than 5 kg N ha^{-1} annually. By contrast, the increase in the average rate of N deposition onto tropical and SH temperate ecosystems was more modest for the contemporary compared to the pre-industrial scenario. The MOGUNTIA simulations demonstrate a tremendous increase in global total N deposition over the last century and a half corresponding to the expansion of industrialization, per capita consumption of N, agriculture, and the world population.

For both the pre-industrial and contemporary N deposition scenarios, the range of N deposition onto an ecosystem or vegetation type often spanned an order of magnitude (Appendix 1, Tables 1 and 2). The range in deposition rates was much narrower when a vegetation type covered less than 20 million hectares within a latitudinal band. Because the lifetime of many reactive nitrogen species is relatively short, hours to days for NH_3, 4.5 days for NH_x (Dentener & Crutzen 1994), and one day for NO_x (Prather et al. 1995), a large fraction of the N tends to be deposited near the location where it was emitted. Some grid cells containing a specific vegetation type were located near modeled sources while others were remote. The distribution of sources and atmospheric dynamics thus determine the amount of N an ecosystem receives through deposition. The vegetation type itself influences the amount of N scavenged from the atmosphere via deposition velocity (see Equation 1). Vegetation may also influence deposition via emission. Some vegetation types, like savannas, emit a great deal of NO_x via soil emission and biomass burning, and the NO_x generated is mostly deposited back onto a savanna, since the lifetime of NO_x and its reaction products are rather short. Intensity of emission, and vegetation interact with the short lifetime of these gases to generate the within biome variability demonstrated by this coarse resolution model. The simulated average rates of deposition onto the biomes should be considered against this background of high spatial variability.

Model/measurement comparison

Globally, modeled and measured rates of N wet deposition were often different. Modeled NO_3^- deposition agreed well with measurements in the United States (Figure 5a). By contrast, the model predicted fluxes of 50% of the measured for NO_3^- fluxes for the European wet deposition data (EMEP) and the compilation of global measurements made by Dentener and Crutzen (1994) (Figures 6 and 7a). Modeled NH_x deposition followed a similar pattern. For the U.S. network, the model predicted wet deposition fluxes of NH_4^+ that were 97% of the measured wet deposition (Figure 4b). However, the model predicted only 43% of the measured deposition for the European network, and only 37% of the measured NH_x deposition for the Dentener and Crutzen (1994) global compilation (Figures 6b and 7b). In addition, the low r^2 for the European (EMEP) NH_x and NO_y comparisons suggests that the model was also unable to capture the correct spatial pattern of wet deposition. These results suggest that model tends to underestimate wet deposition over Europe and in remote areas, but agrees well with wet deposition measurements in the U.S.

Incorrect partitioning of wet and dry deposition may explain some of the discrepancies between the model and measurement data. In Europe, modeled

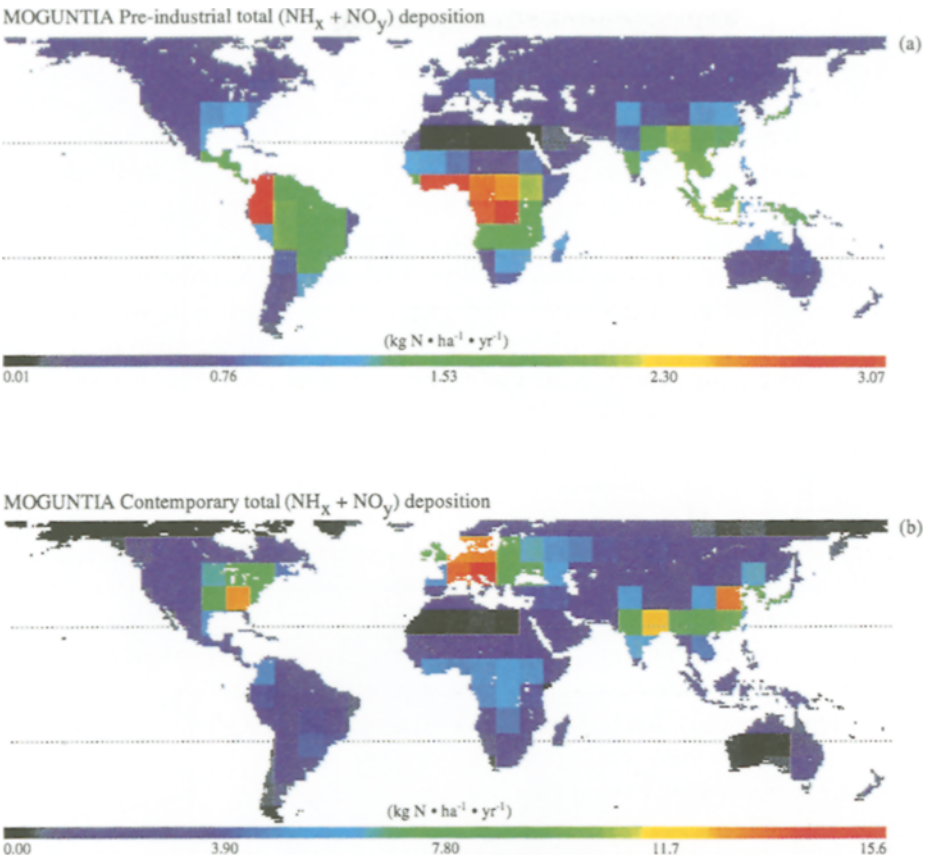

Figure 4. Modeled pre-industrial (a) and contemporary (b) total global N deposition including wet and dry deposition of both NO_y-N and NH_x-N. The results were generated using a model of the troposphere, MOGUNTIA (Dentener & Crutzen 1994).

total deposition of NH_x and NO_y corresponded to bulk precipitation measured deposition (Figure 6a and b). However, bulk deposition measurements of NH_x and NO_3^- are only 4–34% higher than wet-only deposition measurements, because they do not fully capture dry deposition inputs. Thus, differences in methodology offer only a partial explanation of model/measurement discrepancies. To further examine the partitioning of wet and dry deposition, we compared the spatially interpolated wet deposition over Europe and the U.S. with estimated emissions, and the wet and dry deposition fluxes predicted by this coarse resolution model (Table 4). Over both the United States and Europe, dry deposition of NH_x was 50% of total deposition, and dry deposition of NO_y was 65 and 59% of total deposition for the U.S. and Europe, respectively. By comparison, a recent WMO compilation of global deposition measurements found dry deposition of oxidized N (HNO_3 and particulate

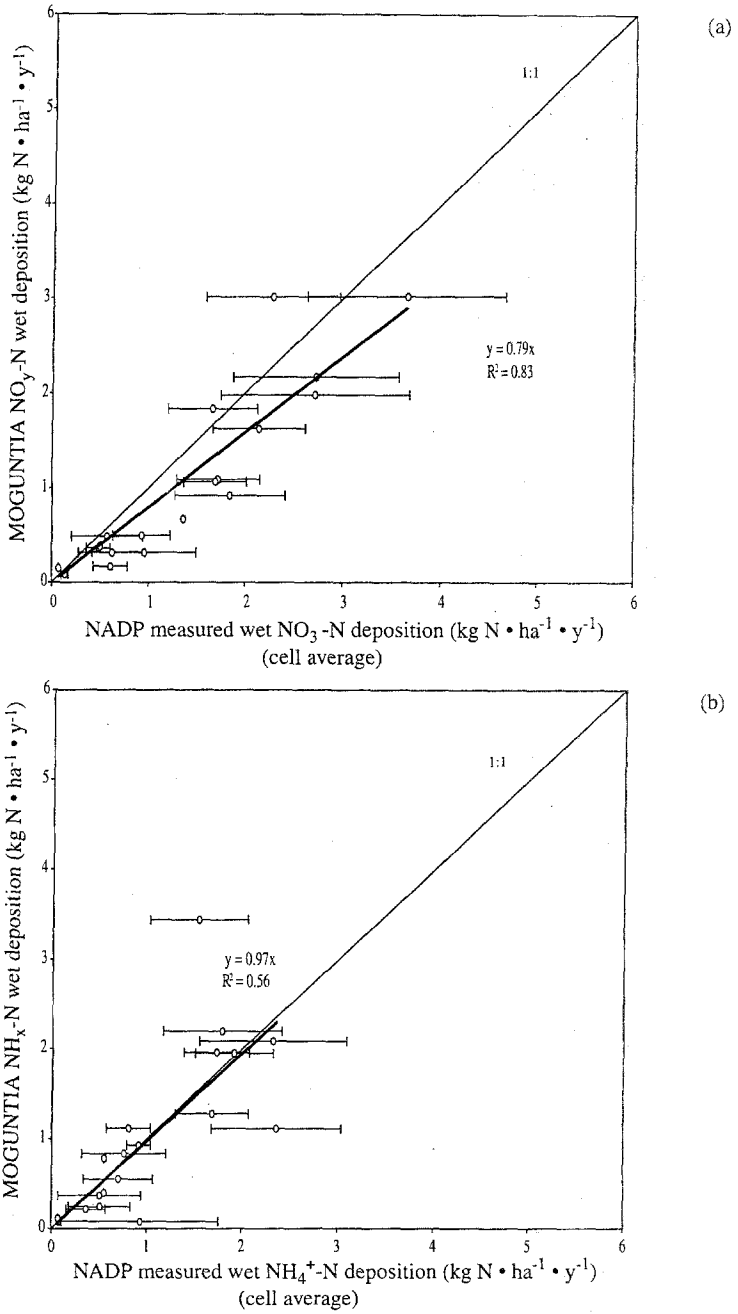

Figure 5. Comparison of simulated NO_y deposition in precipitation with measured wet NO_3^- deposition (a) and of simulated NH_x deposition in precipitation with measured wet NH_4^+ deposition (b) for the United States (NADP/NTN). The bars represent +/– standard deviation of the measured annual N deposition for the sites within a single grid cell. The standard deviation reflects only the spatial variation.

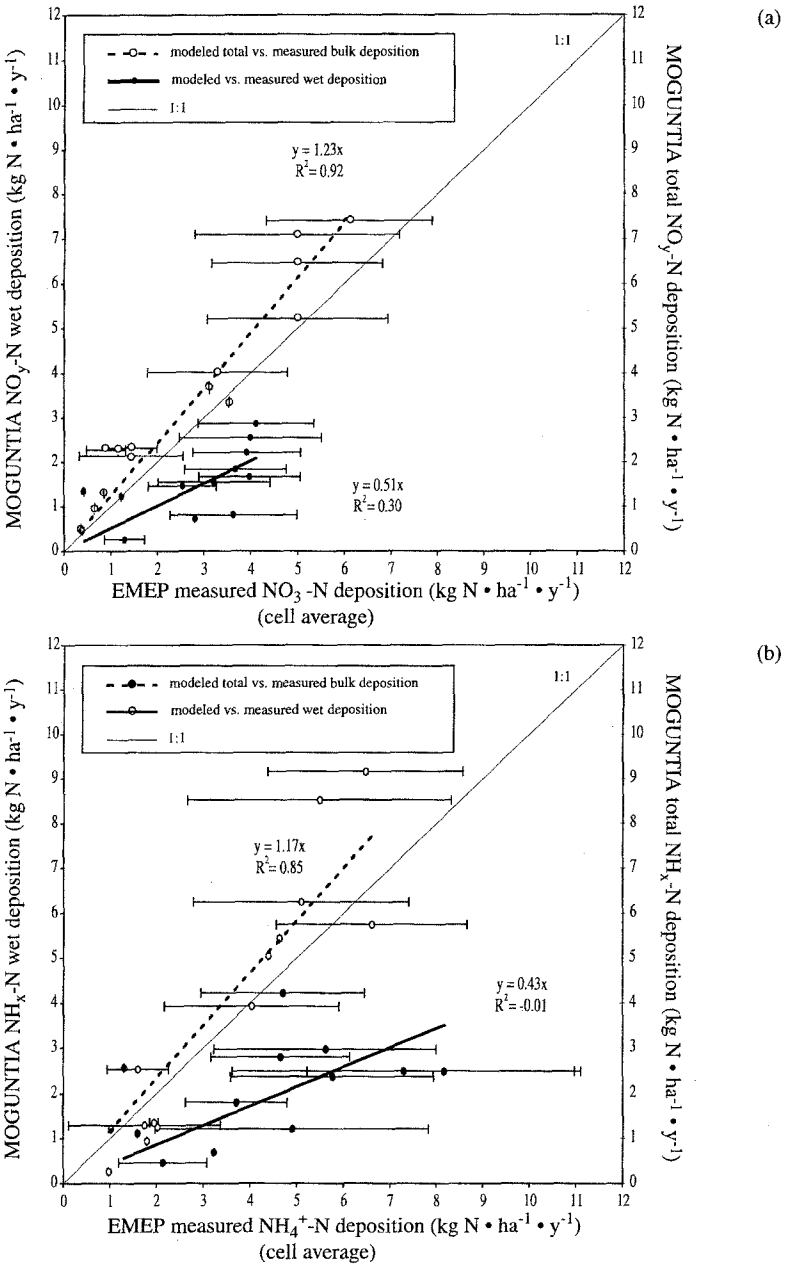

Figure 6. Comparison of European (EMEP) measurements with simulated deposition. (a) Comparison of simulated NO_y wet deposition with measured wet NO_3^- deposition and simulated NO_y wet + dry deposition with measured bulk NO_3^- deposition rates, and (b) Comparison of simulated NH_x wet deposition with measured wet NH_4^+ deposition and simulated NH_X wet + dry deposition with measured bulk NH_4^+ deposition rates. The bars represent +/– standard deviation of the measured annual N deposition for all of the sites within a single grid cell. The standard deviation reflects only the spatial variation.

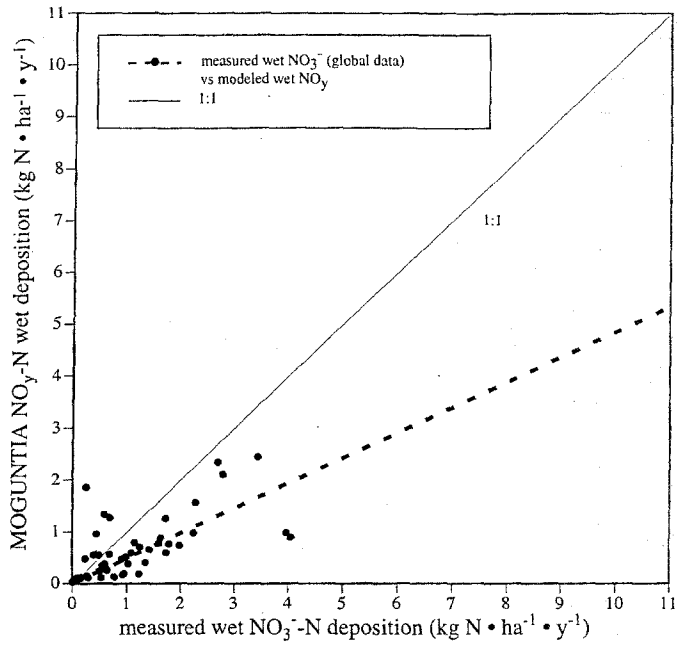

Figure 7. Comparison of simulated NO_y wet deposition, wet + dry NO_y deposition and measured wet NO_3^- deposition (a), and of simulated NH_x wet deposition, wet + dry NH_x deposition total with measured wet NH_4^+ deposition (b) for the compilation of global measurements (Dentener & Crutzen 1994).

Table 4. Spatially integrated emissions, measured wet deposition from NADP/NTN and EMEP, and modeled wet, dry and total deposition. More information on the measurements and integration is provided in the methods section.

	NO_x/NO_y Tg N y^{-1}	NH_3/NH_x Tg N y^{-1}	$NO_x/NO_y + NH_3/NH_x$ Tg N y^{-1}
	United States[1]		
Emissions[2]	6.3	5.2	11.5
Measured wet	1.42	1.18	2.60
Deposition modeled:			
wet deposition	0.94	1.04	1.98
dry deposition	1.72	1.03	2.75
total deposition	2.66	2.07	4.73
	Europe[3]		
Emissions[2]	6.07	5.2	11.27
Measured wet	2.34	3.96	6.30
Deposition modeled:			
wet deposition	1.26	1.81	3.07
dry deposition	1.83	1.85	3.69
total deposition	3.09	3.66	6.76

[1] Land area of the U.S. considered is 7.77 million km^{-2}.
[2] Fossil fuel NO_x emissions are according to Benkovitz et al. 1996 from the NAPAP and EMEP inventories. NH_3 emissions for the U.S. are for all of North and 'Middle' America according to Dentener & Crutzen 1994.
[3] Land area of Europe considered is 8.99 million km^{-2}.

NO_3^-) to be 30–50% of wet + dry oxidized N deposition over the United States, and 20–50% of wet + dry oxidized N deposition over Europe (Whelpdale et al. 1996; Whelpdale et al. 1997). The MOGUNTIA partitioning of wet and dry deposition was more biased toward dry deposition, and likely contributed to the model/measurement data discrepancy for NO_y.

The partitioning hypothesis is consistent with the fact that these MOGUNTIA simulations did not consider deposition of particulate nitrates. There is a growing body of evidence that particulate nitrates (e.g. ammonium nitrate) are present in significant amounts (Erisman & Draaijers 1995). The deposition velocity of particulate nitrate is lower by a factor of 5–10; and hence, wet deposition may be a more important removal mechanism. Underestimation of wet NH_x deposition may be explained by problems in correctly representing the oxidized sulfur cycle in MOGUNTIA, which is usually referred to as the 'oxidant limitation' problem. An underestimate of NH_3

uptake on acidic sulfuric estimate may lead to an increased gas phase NH_3 deposition, and incorrect partitioning of dry and wet deposition fluxes.

Another constraint on our understanding is provided by a look at the total emission and deposition (wet + dry) budgets for the two regions where we have measurements: the U.S. and Europe. Interestingly, estimated NH_3 and NO_x emissions for the U.S. are more than 2 times the total of interpolated wet N deposition for both NH_x and NO_y deposition (Table 4). The Whelpdale et al. 1996 and 1997 compilations suggest that wet deposition in the U.S. (and Europe) is between 50 and 70% of total deposition for oxidized N. Thus, increasing integrated wet deposition by the fraction of dry deposition provides a simple, albeit uncertain, way of estimating total N deposition. Accordingly, the wet + dry oxidized N deposited onto the United States is likely to be between 2.03 and 2.84 Tg NO_y-N y^{-1}. For the reduced species, the picture is somewhat more complicated because the mechanism for atmospheric removal depends on the emissions and the chemical environment (Asman 1994). In areas of high emissions, the dominant removal is via dry deposition, and in areas of low emissions, the dominant removal is via wet deposition (Asman 1994). A single measurement suggests that wet deposition of NH_3 is 70% of total (Harrison & Allen 1991) and model calculations suggest that wet deposition is between 56 and 86% of total deposition (Asman & Van Jaarsveld 1992). Application of these multiplication factors (1/0.56 and 1/0.86) estimate wet + dry reduced N deposition onto the U.S. to be between 1.37 and 2.11 Tg NH_x-N y^{-1}. Thus, we estimate total wet + dry N deposition onto the United States, including both oxidized and reduced N species, to be between 3.40 and 4.95 Tg N y^{-1}.

In the U.S., spatially interpolated total (wet + dry) deposition measurements are only 30–43% of the estimated emitted N, and modeled total deposition onto the U.S. is only 53% of the emitted N. Simulated deposition is sensitive to emission estimates (Dentener & Crutzen 1993; Dentener & Crutzen 1994; Holland et al. 1997b; Holland & Lamarque 1997a). As pointed out above, the emission estimates themselves are uncertain. For example, Bouwman et al. 1997 estimates U.S. NH_3 emissions to be 3.6 Tg NO_x-N y^{-1} compared to the 5.2 Tg NH_x-N y^{-1} used in these simulations. The imbalance between estimated N emissions and deposition measurements may be explained by off-shore deposition of N. Using a simple model, Whelpdale and Galloway (1994) argue that the U.S. exports 0.8–1.2 Tg of oxidized N onto the North Atlantic. A more recent of estimate of the deposition onto the North Atlantic Ocean (excluding the continental shelf) is higher at 4.3 Tg N with deposition onto the Caribbean estimated to be another 4.3 Tg N (Prospero et al. 1996). Inclusion of offshore export places total N deposition within the uncertainty of the estimated emissions. An additional explanation

may be that the measurement sites are located far from urban centers and thus do not reflect the substantial impact that cities and metro-agro-plexes have on regional N deposition patterns (Chameides et al. 1994). The most likely scenario is that off-shore transport, uncertainties in emissions, and the representativeness of the sites together contribute to the calculated imbalance in the U.S. N deposition/emission budget.

Estimated NH_3 emissions for Western Europe are 1.24 Tg N greater than the interpolated NH_x wet deposition measurements. Consistent with the grid cell comparisons of Europe, modeled NH_x wet deposition is less than half of the interpolated NX_x wet deposition (Table 4). Using the same procedure described for estimation of US total NH_x deposition, wet + dry NH_x deposition onto Europe is between 4.60 and 7.07 Tg NH_x-N y^{-1}. Estimated NH_3 emissions balances estimates of wet + dry NH_x deposition within the uncertainty of each. Emissions of oxidized N exceed wet + dry oxidized N deposition estimates of 3.34–4.68 Tg NO-N y^{-1} (calculating using the procedure outlined for the U.S. The inclusion of the bulk precipitation measurements may also contribute to balancing the emissions and deposition budgets. Moreover, European wet deposition measurement sites may capture some of the urban influence missed in the U.S. because the population density is so much greater in Europe. In Europe, oxidized and reduced N emissions come much closer to balancing N deposition given the substantial uncertainties, and suggests that Europe exports much less of its N than does the U.S.

Conclusions

The magnitude and spatial distribution of N deposition has changed substantially over the last 150 years. The greatest rates of pre-industrial N deposition were in the tropics, while contemporary rates of N deposition are highest in NH temperate ecosystems. Some NH temperate ecosystems, cultivated lands and mixed forest, receive 16 times more N now than they did before industrialization, but the average increase in N deposition over NH temperate ecosystems was four-fold. The fate of deposited N varies with ecosystem type and degree of N loading. Contemporary NH temperate forests are able to retain between 20 and 100% of the deposited N depending on the history of N deposition, land use history, and soil texture (Aber & Driscoll 1997; Gosz & Murdoch 1998; Nadelhoffer et al. in press; Nadelhoffer et al. 1995). The NH grasslands and tundra are able to retain between 50 and 100% of the deposited N, an ever greater proportion than forests (Gosz & Murdoch 1998). The ability of cultivated lands to retain nitrogen is limited because the only storage reservoir for nitrogen is soil organic matter which often declines with

cultivation. Furthermore, agricultural lands are fertilized with N and may not be able to retain the additional deposited N because these ecosystems are already saturated with N (Holland 1997b; Townsend 1996). On cultivated lands, the remainder of the nitrogen is removed through harvest, returned to the atmosphere through trace gas production, or lost to groundwater, streams, rivers, and oceans through runoff and leaching. The observation that large quantities of N are deposited onto a relatively small area of cultivated lands may partially explain the strong correlation between NO_y deposition and riverine N fluxes (Howarth et al. 1996; Howarth, this issue).

Our comparisons of measured and modeled deposition suggest that global N deposition modeled by the Dentener and Crutzen 3-D chemical transport model (1993 and 1994) may under-estimate deposition in some regions when compared to measurements. Furthermore, examination of the U.S. and European N emission/deposition budgets point out important imbalances. In the U.S., estimated emissions exceed interpolated total deposition by 3–6 Tg N, suggesting that substantial N is transported offshore and/or the remote and rural location of the sites may fail to capture the deposition of urban emissions. In Europe, interpolated total N deposition came much closer to balancing emissions. Comparison of regional and global modeled deposition with the available measurements will continue to provide critical tests of our understanding of global and regional N cycles.

Acknowledgements

The authors are grateful to Elizabeth Sulzman, A. R. Townsend and two anonymous reviewers for their thoughtful and helpful comments. R. Staufer assisted with figure and manuscript preparation. E. A. Holland is also grateful to A. R., K. E. and D. S. Schimel who assisted with the completion of the manuscript. The work was funded by the Methods and Models for Integrated Assessment Program (MMIA) of the National Science Foundation, grant # ATM 9793346, the National Center for Atmospheric Research, and the Max-Planck-Institute für Biogeochemie. The National Center for Atmospheric Research is operated by the University Corporation for Atmospheric Research under the sponsorship of the National Science Foundation.

Appendix 1, Table 1. Pre-industrial N deposition (NH_x + NO_y) onto potential natural vegetation (Cramer 1995) for Northern Hemisphere (NH) temperate latitudes, tropical latitudes and Southern Hemisphere (SH) temperate latitudes. Deposition was simulated by MOGUNTIA (Dentener and Crutzen 1994). The surface emissions of NH_3 and NO_x used in the simulations are described in Tables 1 and 2. Nitrogen deposition onto individual biomes is summarized in Table 3. The biome classifications are grasslands – G, forests – F, wetlands and riparian zones – W, and mixed life forms – M. Zonal summaries of NO_y, NH_x and NO_y + NH_x deposition are also included. The numbering of the vegetation types follows the numbers assigned by Defries and Townshend 1994.

Vegetation type (biome classification)	NH temperate latitudes			Tropical latitudes			SH temperate latitudes		
	Average deposition kg N ha^{-1} (range)	N deposition Gg (10^9)	Area $ha^{-1} * 10^6$	Average deposition kg N ha^{-1} (range)	N deposition Gg (10^9)	Area $ha^{-1} * 10^6$	Average deposition kg N ha^{-1} (range)	N deposition Gg (10^9)	Area $ha^{-1} * 10^6$
1. Ice	0.37 (0.22–1.12)	**18.27**	*47.22*				0.42 (0.17–0.58)	**0.84**	*1.99*
2. Polar Desert/ Alpine Tundra (G)	0.60 (0.21–2.13)	**214.4**	*311.94*	1.39 (0.84–3.08)	**45.70**	*32.62*	0.68 (0.16–0.84)	**31.75**	*45.7*
3. Wet/Moist Tundra (G)	0.39 (0.21–2.13)	**123.69**	*262.79*	2.93 (2.93–2.93)	**0.90**	*0.31*	0.17 (0.11–0.24)	**0.77**	*4.49*
4. Boreal Forest (F)	0.50 (0.24–2.13)	**637.44**	*1234.9*				0.34 (0.16–0.58)	**1.26**	*3.61*
5. Forested Boreal Wetland (W)	0.50 (0.32–0.73)	**4.48**	*8.25*				0.24 (0.16–0.58)	**3.54**	*14.48*
6. Boreal Woodland (M)	0.38 (0.21–0.84)	**198.67**	*519.87*	1.55 (0.84–3.08)	**36.58**	*23.54*			
7. Non-forested Boreal Woodland (M)	0.46 (0.21–0.84)	**28.79**	*62.40*						

8. Temperate Mixed Forest (F)	0.81 (0.16–2.13)	**427.33**	*520.26*	2.46 (0.84–3.08)	**19.61**	*7.92*	0.84 (0.84–0.84)	**1.64**	*1.96*
9. Temperate Coniferous Forest (F)	0.69 (0.16–2.13)	**165.87**	*227.73*	1.14 (0.56–1.90)	**25.89**	*22.71*	0.49 (0.44–0.58)	**0.35**	*0.72*
10. Temperate Deciduous Forest (F)	0.74 (0.39–1.90)	**266.49**	*351.15*	1.96 (1.06–3.08)	**20.86**	*10.60*	0.46 (0.17–0.58)	**3.32**	*7.24*
11. Temperate Forested Wetland (W)	0.97 (0.89–1.08)	**15.11**	*15.55*						
12. Tall/Medium Grassland (G)	0.67 (0.15–1.12)	**160.69**	*235.61*	1.60 (0.34–2.56)	**80.53**	*50.18*	1.09 (0.30–1.61)	**87.52**	*79.57*
13. Short Grassland (G)	0.56 (0.16–2.13)	**222.91**	*389.71*	0.72 (0.28–1.05)	**22.68**	*31.44*	0.78 (0.28–1.25)	**41.92**	*54.11*
14. Tropical Savanna (M)	0.76 (0.34–1.08)	**153.69**	*235.61*	1.47 (0.07–2.93)	**1829.5**	*1242.5*	1.14 (0.34–1.61)	**141.33**	*124.16*
15. Arid Shrubland (M)	0.48 (0.06–1.12)	**344.42**	*707.02*	0.78 (0.08–3.08)	**284.10**	*360.29*	0.47 (0.16–1.38)	**192.45**	*409.89*
16. Tropical Evergreen Forest (F)	1.85 (0.83–2.13)	**86.17**	*46.44*	2.03 (0.17–3.08)	**3459.28**	*1700.48*	1.28 (0.57–1.61)	**43.49**	*33.86*
17. Tropical Forested Wetland (W)	1.02 (1.02–1.02)	**0.27**	*0.27*	2.50 (0.98–2.93)	**136.84**	*54.6*			
18. Tropical Deciduous Forest (F)	1.32 (0.48–2.13)	**80.33**	*60.61*	1.44 (0.34–3.08)	**573.40**	*396.62*	1.43 (0.84–1.61)	**18.46**	*12.95*

19. Xeromorphic Forest/Woodland (M)	0.67 (0.19–1.12)	**53.69**	*79.70*	1.32 (0.17–3.08)	**617.83**	*466.14*	0.68 (0.21–1.61)	**95.75**	*140.34*
20. Tropical Forested Floodplain (W)				2.21 (1.67–3.08)	**33.39**	*15.121*	1.25 (1.25–1.25)	**0.32**	*0.26*
21. Desert (G)	0.26 (0.06–1.12)	**157.43**	*622.00*	0.43 (0.06–3.08)	**227.47**	*529.90*	0.44 (0.21–0.84)	**7.05**	*16.00*
22. Tropical Non-forested Wetland (W)	0.86 (0.86–0.86)	**0.24**	*0.28*	1.29 (0.68–1.50)	**6.89**	*5.36*			
23. Tropical Non-forested Floodplain (W)	1.46 (0.16–0.16)	**4.14**	*2.83*	1.67 (1.00–2.56)	**55.30**	*32.96*			
24. Temperate Non-forested Wetland (W)	0.59 (0.16–0.96)	**3.26**	*5.50*	1.90 (0.37–3.08)	**52.53**	*27.34*	0.92 (0.69–1.25)	**0.74**	*0.80*
25. Temperate Forested Floodplain (W)	0.47 (0.23–0.75)	**3.78**	*8.19*				1.06 (0.69–1.25)	**2.45**	
26. Temperate Non-forested Floodplain (W)	0.59 (0.15–0.75)	**4.62**	*7.81*				0.57 (0.28–1.25)	**1.24**	*2.16*
27. Wet Savanna (M)	0.86 (0.86–0.86)	**1.68**	*1.96*	1.20 (0.84–1.87)	**2.44**	*2.02*	1.38 (0.69–1.61)	**17.04**	*12.33*
28. Salt Marsh (W)	0.90 (0.27–1.08)	**3.80**	*4.16*	1.41 (0.84–1.99)	**1.64**	*1.16*	0.77 (0.69–0.84)	**3.13**	*4.06*

29. Mangrove (W)				1.82 (0.79–2.93)	**21.18**	*11.60*			
31. Temperate Savanna (M)	0.55 (0.07–1.90)	**341.10**	*626.84*	0.80 (0.80–0.80)	**0.23**	*0.28*	0.64 (0.38–0.80)	**39.77**	*62.22*
33. Temperate Broad-leaved Evergreen Forest (F)	1.29 (0.16–2.13)	**260.63**	*198.39*	2.05 (0.60–3.08)	**85.63**	*41.58*	0.51 (0.30–0.80)	**49.32**	*94.57*
35. Mediterranean Shrubland (M)	0.43 (0.07–0.60)	**39.62**	*93.26*				0.48 (0.33–0.81)	**25.79**	*54.13*
Zonal Σ of NH_x deposition on land	0.30 (0.02–1.06)	**2067**	*6673*	0.63 (0.02–1.77)	**3219**	*5068*	0.40 (0.07–0.87)	**474.4**	*1184*
Zonal Σ of NO_y deposition on land	0.25 (0.03–1.27)	**1817**	*6673*	0.86 (0.03–1.95)	**4421**	*5068*	0.28 (0.04–0.79)	**337.9**	*1184*
Zonal Σ of NH_x + NO_y deposition on land	0.55 (0.06–2.13)	**3885**	*6673*	1.49 (0.06–3.08)	**7640**	*5068*	0.67 (0.11–1.61)	**811.2**	*1184*

Appendix 1, Table 2. Contemporary N deposition (NH_x + NO_y, and wet plus dry deposition) onto the Defreis and Townsend land cover classification (DeFries and Townsend 1994) for Northern Hemisphere (NH) temperate latitudes, tropical latitudes and Southern Hemisphere (SH) temperate latitudes. Deposition was simulated by MOGUNTIA (Dentener and Crutzen 1994). The surface emissions of NH_3 and NO_x used in the simulations are describe in Tables 1 and 2. Nitrogen deposition onto individual biomes is summarized in Table 3. The biome classifications are grasslands – G, forests – F, cultivated lands – C, and mixed life forms – M. Zonal summarizes of NO_y, NH_x and NO_y + NH_x deposition are also included. The numbering of the vegetation types follows the numbers assigned by Defries and Townsend (1994).

Vegetation type (biome classification)	NH temperate latitudes			Tropical latitudes			SH temperate latitudes		
	Average N deposition kg N ha^{-1} (range)	N deposition Gg (10^9)	Area $ha^{-1} * 10^6$	Average N deposition kg N ha^{-1} (range)	N deposition Gg (10^9)	Area $ha^{-1} * 10^6$	Average N deposition kg N ha^{-1} (range)	N deposition Gg (10^9)	Area $ha^{-1} * 10^6$
1. Broadleaf Evergreen Forest (F)				3.34	**4475.8**	*1345*			
2. Broadleaf Deciduous Forest and Woodland (F)	6.81 (0.51–15.6)	**1093**	*156*	3.24 (0.36–9.21)	**457**	*142*	1.26 (0.45–4.16)	**41.8**	*32.9*
3. Mixed Coniferous and Broadleaf Deciduous Forest and Woodland (F)	7.59 (0.99–15.6)	**4652**	*598*	4.16 (0.39–12.5)	**4.7**	*1.1*	2.13 (0.51–4.16)	**136**	*62.2*
4. Coniferous Forest and Woodland (F)	2.34 (0.29–15.6)	**2916**	*1182*				0.89 (0.33–1.38)	**8.05**	*8.74*
5. High latitude Deciduous Forest and Woodland (F)	1.45 (0.29–6.43)	**813**	*539*						

6. & 8. Wooded C4 Grassland (M)	8.82 (3.06–13.3)	**1739**	*197*	3.98 (0.45–12.5)	**5381**	*1354*	2.70 (0.91–4.16)	**439**	*162*
7. C4 Grassland (G)	5.14 (0.66–13.3)	**986**	*190*	2.70 (0.39–12.5)	**1701**	*630*	2.14 (0.67–3.55)	**162**	*75.0*
9. Shrubs and Bare Ground (M)	2.74 (0.29–13.3)	**1047**	*380*	1.46 (0.29–8.04)	**454**	*307*	0.92 (0.24–3.55)	**381**	*414*
10. Tundra (G)	0.88 (0.29–13.3)	**269**	*293*						
11. Desert Bare Ground (G)	1.73 (0.29–8.04)	**1607**	*941*	1.45 (0.29–3.93)	**992**	*679*	1.19 (0.03–3.55)	**53.7**	*454*
12. Cultivation (C)	7.42 (0.59–15.6)	**6605**	*878*	4.15 (0.36–12.5)	**1302**	*316*	1.54 (0.47–4.16)	**212**	*136*
13. Ice (I)	0.55 (0.40–0.64)	**15.8**	*28.7*				0.05 (0.03–0.08)	**0.88**	*19.4*
14. C3 Wooded Grassland (M)	7.03 (0.59–15.6)	**1373**	*197*	3.89 (0.45–9.21)	**602**	*155*	1.93 (0.24–4.16)	**221**	*109*
15. C3 Grassland (G)	3.48 (0.34–15.6)	**3531**	*997*	2.64 (0.45–4.89)	**179**	*679*	1.15 (0.24–3.55)	**109**	*89.3*
Zonal Σ of NH_X deposition on land	1.96 (0.11–9.51)	**14150**	*6579*	1.42 (0.15–9.51)	**7063**	*4997*	0.90 (0.01–2.48)	**1070**	*1154*
Zonal Σ of NO_y deposition on land	1.80 (0.12–7.96)	1.69	**12497**	*6579* (0.11–3.75)	**8486**	*4997*	0.57 (0.02–2.09)	**694**	*1154*
Zonal Σ of NH_X + NO_y deposition on land	3.76 (0.29–15.6)	**26647**	*6579*	3.10 (0.29–12.5)	**15549**	*4997*	1.48 (0.03–4.16)	**1764**	*1154*

References

Aber JD & Driscoll CT (1997) Effects of land use, climate variation, and N deposition on N cycling and C storage in northern hardwood forests. Global Biogeochem. Cycles 11: 639–648

Aber JD, Nadelhoffer KJ, Steudler P & Melillo JM (1989) Nitrogen saturation in northern forest ecosystems. BioScience 39: 378–386

Asman WAH & Van Jaarsveld HA (1992) A variable-resolution transport model applied for NH_X in Europe. Atmospheric Environment 26A: 445–464

Asman WH (1994) Emission and deposition of ammonia and ammonium. Nova Acta Leopoldina NF 70: 263–297

Benkovitz CM, Scholtz MT, Pacyna J, Tarrason L, Dignon J, Voldner EC, Spiro PA, Jogan JA & Graedel TE (1996) Global gridded inventories of anthropogenic emission of sulfur and nitrogen. J. Geophys. Res. 101: 29,239–29,253

Bottger KA, Gravenhorst G & Ehhalt DH (1978) Atmospharische Kreislauf von Stickoxiden und Amoniak. In: Kernforschungsanlage Julich, Julich Report number 1558

Bouwman AF, Lee DS, Asman WAH, Dentener FJ, Van Der Hoek KW & Olivier JGJ (1997) A global high-resolution emission inventory for ammonia. Global Biogeochem. Cycles 11: 561–587

Carpenter S, Caraco NF, Corrlee DL, Howarth RW, Sharpley AN & Smity VH (1998) Nonpoint pollution of surface waters with phosphorus and nitrogen. Ecol. App. 8: 559–568

Chameides WL, Kasibhatla PS, Yienger J & Levy II H (1994) Growth of continental-scale metro-agro-plexes, regional ozone pollution, and world food production. Science 264: 74–77

Cleveland CC, Townsend AR, Schimel DS, Howarth RW, Hedin LO, Perakis SS, von Fischer JD, Wasson MF, Latty EF & Elseroad A (submitted) Global patterns of terrestrial biological concentration (N_2) fixation in natural ecosystems. Global Biogeochem. Cycles

Cornell S, Rendell A & Jickells T (1995) Atmospheric inputs of dissolved organic nitrogen to the ocean. Nature 376: 243–246

Cramer W, Claussen M & Solomon AM (1995) An assessment of different climate change scenarios for the global redistribution of agricultural land. First Science Conference, Int. Geosphere-Biosphere Programme, Global Anal., Interpret., and Model, Garmisch-Partenkirchen, Germany

Crutzen PJ & Andreae MO (1990) Biomass burning in the tropics: Impact on atmospheric chemistry and biogeochemical cycles. Science 250: 1669–1678

Crutzen PJ & Gidel LT (1983) A two-dimensional photochemical model of the atmosphere 2: The tropospheric budges of the anthropogenic chlorocarbons CO, CH_4, CH_3Cl and the effect of the various NO_X sources on tropospheric ozone. J. Geophys. Res. 88: 6641–6661

Crutzen PJ & Zimmermann PH (1991) The changing photochemistry of the troposphere. Tellus 43AB: 136–151

Davidson EA & Kingerlee W (1997) Global inventory of nitric oxide emissions from soils. Nutrient Cycling in Agroecosystems 48: 37–50

Dawson GA (1977) Atmospheric amonia from undisturbed land. J. Geophys. Res. 82: 3125–3133

DeFries RM & Townshend JRG (1995) An initial coarse resolution NDVI-derived global land cover classification. In ISLSCP Initiative 1: Global Data Sets for Land/Atmosphere Models 1987–1988. CD-ROM NASA, Greenbelt, Md

Delmas R, Derca D & Jambert C (1997) Global inventory of NO_X sources. Nutrient Cycling in Agroecosystems 48: 51–60

Dentener FJ & Crutzen PJ (1993) Reaction of N_2O_5 on trospheric aerosols: Impact on the global distributions of NO_x, O_3 and OH. J. Geophys. Res. 98: 7149–7163

Dentener FJ & Crutzen PJ (1994) A three-dimensional model of the global ammonia cycle. J. Atmos. Chem. 19: 331–369

Dignon J & Hameed S (1989) Global emission of nitrogen and sulfur oxides from 1960 to 1980. J. Air Poll. Control Assoc. 39: 180–186

Elkund TJ, McDowell WH & Pringle CM (1997) Seasonal variation of tropical precipitation chemistry: La Selva, Costa Rica. Atmos. Environ. 31: 3903–3910

Erisman JW, Beier C, Draaijers G & Lindberg S (1994) Review of deposition monitoring methods. Tellus 46B: 79–83

Erisman JW & Draaijers GPJ (1995) Atmospheric Deposition in Relation to Acidification and Eutrophication. Elsevier Press, New York

Feichter J & Crutzen PJ (1990) Parameterization of vertical tracer transport due to deep cumulus convection in a global transport model and its evaluation of 222 Radon measurements. Tellus, Series B 42: 100–117

Food and Agriculture Organization (1985) 1984 FAO Production Yearbook, Vol. 38, FAO Statistics Series 61, United Nations, Rome

Food and Agriculture Organization (1986) 1985 FAO Fertilizer Yearbook, Vol. 35, FAO Statistics Series 71, United Nations, Rome

Food and Agriculture Organization (1990a) 1989 FAO Production Yearbook, Vol. 43, FAO Statistics Series 100, United Nations, Rome

Food and Agriculture Organization (1990b) 1989 FAO Fertilizer Yearbook, Vol. 39, FAO Statistics Series 95, United Nations, Rome

Food and Agriculture Organization (1991) 1990 FAO Production Yearbook, Vol. 40, FAO Statistics Series 61, United Nations, Rome

Franzblau E & Popp CJ (1989) Nitrogen oxides produced from lightning. J. Geophys. Res. 94: 11,089–11,104

Galbally IE & Johansson C (1989) A model relating laboratory measurements of rates of nitric oxide production and field measurements of nitric oxide emission from soils. J. Geophys. Res. 94: 6473–6480

Galbally IE & Roy CR (1978) Loss of fixed nitrogen from soils by nitric oxide exhalation. Nature 275: 734–735

Galloway JN, Levy HI & Kasibhalta PS (1994) Year 2020: Consequences of population growth and development on deposition of oxidized nitrogen. Ambio 23: 120–123

Galloway JN, Schlesinger WH, Levy HI, Michaels A & Schnoor JL (1995) Nitrogen fixation: Anthropogenic enhancement environmental response. Global Biogeochem. Cycles 9: 235–252

Galloway JN, Dianwu Z, Thomson VE & Chang LH (1996) Nitrogen mobilization in the United States of America and the People's Republic of China. Atmos. Env. 30: 1,551–1,561

Gosz JR & Murdoch P (1998) Integrating the nation's environmental monitoring and research networks and programs: An exercise to demonstrate the value of index areas in a national network. In: Office of Science and Technology Police (OSTP)

Haas TC (1990) Kriging and automated variogram modeling within a moving window. Atmospheric Environment 24A: 1759–1769

Harrison RM & Allen AG (1991) Scavenging ratios and deposition of sulphur, nitrogen, and chlorine species in eastern England. Atmospheric Environment 25A: 1719–1723

Hicks BB (1989) Atmospheric processes research and process model development. In: National Acid Precipitation Assessment Program, NOAA/ATDD, 2

Holland EA, Braswell BH, Lamarque J-F, Townsend A, Sulzman JM, Müller J-F, Dentener F, Brasseur G, Levy HI, Penner JE & Roelofs G (1997b) Variations in the predicted spatial distribution of atmospheric nitrogen deposition and their impact on carbon uptake by terrestrial ecosystems. J. Geophys. Res. 102: 15,849–15,866

Holland EA & Lamarque J-F (1997a) Modeling bio-atmospheric coupling of the nitrogen cycle through NO_x emissions and NO_y deposition. Nutrient Cycling in Agroecosystems 48: 7–24

Howarth RW, Billen G, Swaney D, Townsend A, Jaeorski N, Lajtha K, Downing JA, Elmgren R, Caraco N, Jordan T, Berendse F, Freney J, Kudeyarov V, Murdoch P & Zhao-liang Z (1996) Regional nitrogen budgets and riverine N & P fluxes for the drainages to the North Atlantic Ocean: Natural and human influences. Biogeochemistry 35: 75–139

Jaeger L (1976) Monatskarten des Niederschlags für die ganze Erde. Beri. Dtsch. Wetterdienstes 139:

Kittel TGF, Rosenbloom NA, Painter TH, Schimel DS & Participants VM (1995) The VEMAP integrated database for modeling United States ecosystem/vegetation sensitivity to climate change. J. Biogeography 22: 857

Langford AO, Fehsenfeld FC, Zachariassen J & Schimel DS (1992) Gaseous ammonia fluxes and background concentrations in terrestrial ecosystems of the United States. Global Biogeochem. Cycles 6: 459–483

Lee DS, Kohler I, Grobler E, Rohrer F, Sausen R, Gallardo-Klenner L, Olivier JGJ, Dentener FJ & Bouwman AF (1997) Estimations of global NO_x emissions and their uncertainties. Atmospheric Environment 31: 1735–1749

Leemans R & Cramer WP (1991) The IIASA database for mean monthly values of temperature, precipitation and cloudiness of global terrestrial grid. WP-41. International Institute of Applied Systems Analyses, Laxenvurg, Austria

Levy H, Moxim WJ & Kasibhatla PS (1996a) A global three-dimensional time-dependent lightning source of tropospheric NO_x. J. Geophys. Res. 101: 22,911–22,922

Levy H, Moxim WJ & Kasibhatla PS (1996b) Tropospheric NO_x: Its sources and distribution. J. Geophys. Res. 101: 22,911–22,922

Logan JA (1983) Nitrogen oxides in the troposphere: Global and regional budgets. J. Geophys. Res. 88D: 10,785–10,807

Matthews E (1994) Nitrogenous fertilizers: Global distribution of consumption and associated emissions of nitrous oxide and ammonia. Global Biogeochem. Cycles 8: 411–439

Mayewski PA, Lyons WB, Spencer MJ, Twickler MS, Buck CF & Whitlow S (1990) An ice-core record of atmospheric response to anthropogenic sulfate and nitrate. Nature 346: 554–556

Michaels AF, Siegel DA, Johnson RJ, Knap AH & Galloway JN (1993) Episodic inputs of atmospheric nitrogen to the Sargasso Sea: Contributions to new production and phytoplankton blooms. Global Biogeochem. Cycles 7: 339–351

Muller J-F (1992) Geographical distribution and seasonal variation of surface emissions and deposition velocities of atmospheric trace gases. J. Geophys. Res. 97: 3787–3804

Nadelhofer KJ, Downs MR, Fry B, Magill A & Aber JD (in press) Controls on N retention and exports in a fertilized watershed. Environmental Monitoring and Assessment

Nadelhoffer KJ, Downs Mr, Fry B, Aber JD, Magill AH & Melillo JM (1995) The fate of ^{15}N-labeled nitrate additions to a northern hardwood forest in eastern Maine, U.S.A. Oceanologia 103: 292–301

Neff JC, Keller M, Holland EA, Weitz AW & Veldkamp E (1995) Fluxes of nitric oxide from soils following the clearing and burning of a secondary tropical rain forest. J. Geophys. Res. 100: 25,913–25,922

Newell RE, Kidson JW, Vincent DG & Boer GJ (1974) The General Circulation of the Tropical Atmosphere and Interactions with Extra Tropical Latitudes. MIT Press, Cambridge, Mass

Olivier JGJ, Bouwman AF, van der Maas CWM, Berdowski JJM, Veldt C, Bloos JPJ, Visschedijk AJH, Zandveld PYJ & Havelag JL (1995) Description of EDGAR Version 2.0: A set of global emission inventories of greenhouse gases and ozone-depleting substances for all anthropogenic and most natural sources on a per country basis on 1 × grid. In: RIWM, 771060 002

Oort AH (1983) Global atmospheric circulation statistics, 1958–1973. In: Natl. Oceanic and Atmos. Admin., Report Number 14

Penner JE, Atherton CS, Dignon J, Ghan SJ & Walton JJ (1991) Tropospheric nitrogen: a three dimensional study of sources, distributions and deposition. J. Geophys. Res. 96D: 959–990

Penner JE, Atherton CS & Graedel TE (1994) Global emissions and models of photochemically active compounds. In: Prinn RG (Ed.) Global Atmospheric-Biospheric Chemistry, Plenum Press, New York

Potter CS, Matson PA, Vitousek PM & Davidson EA (1996) Process modeling of controls on nitrogen trace gas emissions from soils worldwide. J. Geophys. Res. 101: 1361–1377

Prather M, Derwent R, Ehhalt D, Fraser P, Sanhueza E & Zhou X (1995) Other Trace Gases and Atmospheric Chemistry. In: Climate Change 1994, Radiative Forcing of Climate Change. Intergovernmental Panel on Climate Change (pp 73–126). Cambridge University Press, Cambridge

Price C, Penner J & Prather M (1997a) NO_X from lightning, 1, Global distribution based on lightning physics. J. Geophys. Res. 102: 5929–5941

Price C, Penner J & Prather M (1997b) NO_X from lightning, 2, Constraints from the global atmospheric electric circuit. J. Geophys. Res. 102: 5943–5951

Prospero JM, Barrett K, Church T, Dentener F, Duce RA, Galloway JN, Levy II H, Moody J & Quinn P (1996) Atmospheric deposition of nutrients to the North Atlantic Basin. Biogeochemistry 35: 27–73

Rendell AR, Ottley CJ, Jickells TD & Harrison RM (1993) The atmospheric input of nitrogen species to the North Sea. Tellus 45B: 53–63

Ridley BA & Atlas E (in press, anticipated publication January 1999) Nitrogen Compounds. In: Brasseur GP, Orlando JJ & Tyndall GS (Eds) Atmospheric Chemistry and Global Change. Oxford University Press, New York

Ridley BA, Dye JE, Walega JG, Zhenge J, Grahek FE & Rison W (1996) On the production of active nitrogen by thunderstorms over New Mexico. J. Geophys. Res. 101: 20,985–21,005

Sanhueza E, Fraser PJ & Zander RJ (1995) Scientific assessment of ozone depletion 1994: Source gasses: Trends and budgets. In: World Meterological Organization, 37

Schimel D, Braswell BH, McKeown R, Ojima DS, Parton WJ & Pulliam W (1996) Climate and nitrogen controls on the geography and timescales of terrestrial biogeochemical cycling. Global Biogeochem. Cycles 10: 677–692

Schimel DS, Braswell BH & Parton WJ (1997) Equilibration of the terrestrial water, nitrogen, and carbon cycles. Proceedings of the National Academy of Sciences 94: 8280–8283

Schlesinger WH & Hartley AE (1992) A global budget for atmospheric NH_3. Biogeochemistry 15: 191–211

Schulze ED (1989) Air pollution and forest decline in a spruce (Picea Abies) forest. Science 244: 776–783

Setzer AW & Pereira MC (1991) Amazonia biomass burnings in 1987 and an estimate of their tropospheric emissions. Ambio 20: 19–22

Soderlund R & Svensson BH (1976) Their global nitrogen cycle. Nitrogen, Phosphorous and Sulphur Global Cycles SCOPE 7: 23–73

Stedman DH & Shetter RE (1983) The global budget of atmospheric nitrogen species. In: Schwartz SE (Ed.) Trace Atmospheric Constituents (pp 411–454). John Wiley & Sons, New York

Stohl A, Williams E, Wotawa G & Kromp-Kolb H (1996) A European inventory of soil nitric oxide emissions and the effect of these emissions on the photochemical formation of ozone. Atmos. Env. 30: 3,741–3,755

Sulzman J, Braswell BH, Holland EA & Lamarque JF (1997) Poster: A Comprehensive Compilation of Atmospheric Deposition Data for Global and Regional Studies. Ecological Society of America, Albuquerque, NM

Townsend AR, Braswell BH, Holland EA & Penner JE (1996) Spatial and temporal patterns in potential terrestrial carbon storage resulting from deposition of fossil fuel derived nitrogen. Ecological Applications 6: 806–814

Van Breemen N, Bottough PA, Velthorst EJ, Van Dobben HF, De Wit T, Ridder TB & Reunders HF (1982) Soil acidification from atmospheric ammonium sulfate in forest canopy throughfall. Nature 299: 548–550

Veldkamp E & Keller M (1997) Fertilizer induced nitric oxide emissions from agricultural soils. Nutrient Cycling in Agroecosystems 48: 69–77

Vitousek PM, Aber JD, Howarth RW, Likens GE, Matson PA, Schindler DW, Schlesinger WH & Tilman DG (1997) Human alteration of the global nitrogen cycle: sources and consequences. Ecol. Appl. 7: 737–750

Wagenbach D, Munnich KO, Schotterrer U & Aeschger H (1988) The anthropogenic impact on snow chemistry at Colle Gnifetti, Swiss Alps. Ann. Glaciol. 10: 183–187

Warneck P (1988) Chemistry of the Natural Atmosphere. Academic Press, San Diego

Wesely ML (1989) Parameterization of surface resistance to gaseous dry deposition in regional-scale numerical models. Atmospheric Environment 23: 1293–1304

Whelpdale DM, Dorling SR, Hicks BB & Summers PW (1996) Atmospheric Processes. In: World Meterological Organizational Global Atmosphere Watch: Global Acid Deposition Assessment, 106

Whelpdale DM & Galloway JN (1994) Sulphur and nitrogen oxide fluxes in the North Atlantic atmosphere. Global Biogeochem. Cycles 8: 481–493

Whelpdale DM, Summers PW & Sanhueza E (1997) A global overview of atmospheric acid deposition fluxes. Environmental Monitoring and Assessment 48: 217–227

Williams EJ, Guenther A & Fehsenfeld FC (1992) An inventory of nitric oxide emissions from soils in the United States. J. Geophys. Res. 97: 7511–7519

Yienger JJ & Levy II H (1995) Empirical model of global soil-biogenic NO_x emissions. J. Geophys. Res. 100: 11,447–11,464

Zimmermann PH (1987) MOGUNTIA: A handy global tracer model. Proceedings of the Sixteenth NATO/CCMS International Technical Meeting on Air Pollution Modeling and Its Application, New York